1. Mohammad Tariq NASIR[1], 2. Nabil BEITHOU[1,2], 3. Gabriel BOROWSKI[3], 4. Sameh ALSAQOOR[2]

Applied Science Private University, Amman, Jordan (1), Tafila Technical University, Tafila, Jordan (2),
Lublin University of Technology, Lublin, Poland (3).
ORCID: 1. 0000-0001-6625-8272; 2. 0000-0002-3283-1402; 3. 0000-0001-6971-5395; 4. 0000-0002-0552-8926

doi:10.15199/48.2022.08.15

Simulation studies of controllers for battery thermal management system with multi-thermoelectric modules

Abstract. *In this paper, an simulated investigations for the modified lithium-ion battery thermal management system using PID, as well Null-Space-based Behavioral (NSB) controllers were presented. This work sought to keep the battery life at its optimum temperature using low power. We used thermoelectric modules with collaborating controllers to minimize the electricity consumed during the cooling process. Comparing to PID, NSB controller achieved the reduction of consumed power of 20%, faster temperature return to the set point, and a more uniform controlling the temperature of the battery cells.*

Streszczenie. *W niniejszym artykule przedstawiono wyniki symulacyjnych badań nad zmodyfikowaniem systemu zarządzania temperaturą akumulatora litowo-jonowego z wykorzystaniem regulatora PID oraz regulatora behawioralnego typu Null-Space (NSB). Celem pracy było utrzymanie żywotności baterii w optymalnej temperaturze przy niskim poborze mocy. Wykorzystano moduły termoelektryczne z dedykowanym sterownikiem dla zmniejszenia zużycia energii elektrycznej podczas procesu chłodzenia. W porównaniu do PID, zastosowanie regulatora NSB umożliwia redukcję pobieranej mocy o 20%, szybszy powrót temperatury do wartości zadanej oraz bardziej równomierne sterowanie temperaturą ogniw akumulatora.* (***Badania symulacyjne kontrolerów systemu zarządzania temperaturą akumulatora z modułami multi-termoelektrycznymi***)

Keywords: thermoelectric module, electric vehicles, battery thermal management system
Słowa kluczowe: moduł termoelektryczny, pojazdy elektryczne, system zarządzania temperaturą akumulatora

Introduction

Transportation represents 26% of the total energy consumed [1]; huge amounts of CO_2 emissions are produced from vehicles. Electric vehicles (EV) are expected to increase from around 5% of global car sales to more than 60% by 2030 [2, 3]. The technology of electric vehicles is well-known, only batteries are needed to be improved in terms of safety, reliability and lifespan. Most of these problems are associated with the heat generation-dissipation in charging and discharging of the battery [4]. The battery capacity, power, self-discharge, thermal runaway and electrical balances are all problems need to deal with to improve batteries. The non-uniform temperature distribution highly affects the performance and lifespan of the batteries [5, 6]. Different types of high energy power EV batteries are tested, such as nickel-metal-hydride (Ni-MH), lithium-ion (Li-ion), lithium-titanate and proton exchange membrane fuel cells (PEMFCs). Such batteries are used in pure electric vehicles, hybrid electric vehicles (HEV) and fuel cell electric vehicles (FCEV) [7, 8]. The most used batteries in EVs are Li-ion batteries, due to their energy density. Heat dissipation issue is a main problem in lithium-ion batteries; it affects power, life and safety of the used battery [9]. Researchers dealt with the cooling problem of Li-ion batteries in different ways, air or liquid forced convection heat transferred were used to cool down the battery cells [10], the non-uniform temperature distribution is treated by phase change material to dissipate the max power, as in [11-13]. Phase change composite materials offer passive protection at low weight and cost while minimizing system complexity for a Li-ion pack batteries for small electric vehicles [14]. Liquid metal, nanofluids and ammonia were all used to reduce the temperature of the batteries to keep it at about its optimum operation condition; all studies were able to dissipate the heat at a certain time and reach the range of optimal working conditions of the batteries even as low as 7 °C if required [15-17]. Heat dissipation configurations are also analyzed at different levels, the series cooling and parallel cooling. It was found, that the parallel configuration makes better temperature distribution in the battery [18, 19]. Double copper mesh-phase change material plate heat dissipation method provides an efficient solution for the thermal management of rectangular battery modules. At high temperature and discharge rate conditions, HEV and plug-in electrical vehicles (PEV) batteries may not work normally, unless they are matched with an effective battery thermal management system (BTMS) [20]. To build an accurate BTMS, solid state cooling is favorited for its controllable heat dissipation and low temperature may reach. Solid state cooling depends on thermoelectric modules (TEMs) adjusted on the battery boundaries and forced air circulation [21]. Recently, the researchers started concentrating on using TEMs as the heat dissipation device; mathematical modeling, numerical solution and simulation using ANSYS 17 have been performed [22-24]. To have accurate temperature throughout the battery, controllers must be included. Microcontroller based thermoelectric cooler was proposed, achieving fast and reasonable cooling [25].

Higher battery life and performance are achieved around the operating temperatures 20−40 °C. Li-ion batteries produce heat while charging and discharging due to enthalpy changes, electrochemical polarization and resistive heating inside the cell. This prevents the battery temperature from achieving optimal conditions, leading to a shorter lifespan of batteries and lower performance. Different types of BTMS based on the cooling method are used: air cooling and heating, liquid cooling and heating, composite phase change and thermoelectric systems [26-30].

Recent experiments applied TEM for BTMS [31]. Traditional experimental systems consist of heating source for simulating the battery heat generation during charging and discharging, surrounded by cooling fluid which absorb the heat generated, then pumped into a heat exchanger attached with the cold side of TEM. Such systems consume power in running the electrical pump and in TEM cooling power. To reduce the power consumed during the BTM process, multi-TEMs were attached

directly to the battery liquid tank, and controlled by a Null-Space-based Behavioral (NSB) controller [32].

The goal of this work was to keep the battery at its optimum temperature using low power. To achieve it, the thermoelectric modules with collaborating controllers to minimize the electricity consumed during the cooling process was implemented.

a)

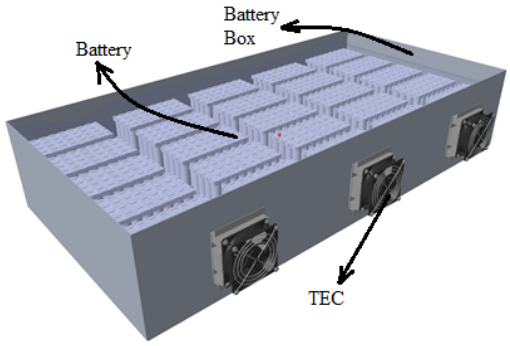

b)

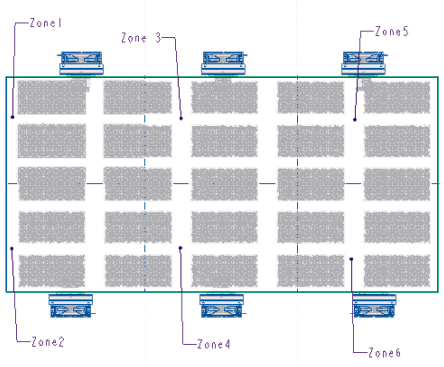

Fig. 1. System used in battery thermal management: a) battery box with TEMs, b) battery box top view divided into six zones

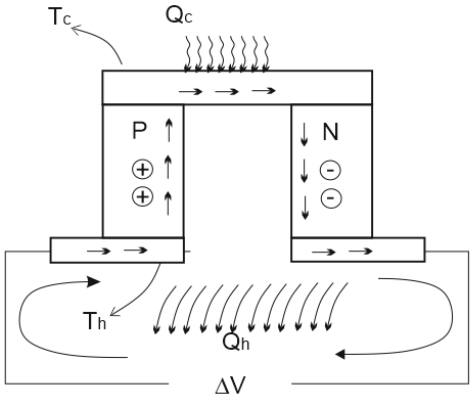

Fig. 2. Schematic diagram of the thermoelectric cooler: P, N – junctions, T_c – cold side temperature, T_h – hot side temperature, Q_c – heat absorbed from the hot side, Q_h – heat rejected at the cold side of TEM

Methodology

The methodology based on cooling lithium-ion battery using multi-TEMs with the assistance of a NSB controlling unit to minimize the energy consumed during heat addition or removal from battery. The BTMS consists of a battery box, TEM, controller and sensors as shown in Figure 1. The battery box was divided into six compartments (zones); each compartment was attached with a TEM. The TEMs (Figure 2) are solid state semiconductor devices, with no moving parts; which makes them rugged, reliable, and quiet. TEMs are environmental friendly alternative to vapour-compression refrigeration. They can be extremely compact and allow precise temperature control (< ±0.1 °C) with precise current supply. TEMs have the best coefficient of performance at a specified current. It can be controlled by different methods to minimize the energy used, such as PID controller [33], NSB controller [34] or other.

Mathematical model

To perform the mathematical model of the system, the battery box was divided into six zones, as shown in Figure 1b, each zone has the following governing equations.

General energy conservation:

$$\dot{E}_{in} - \dot{E}_{out} + \dot{E}_{gen} = \frac{dE}{dt}\Big|_{CV}$$

For each compartment from 1-6 as:

(1) $$\rho\, V\, c_p\, \frac{dT_1}{dt} = 2\,\frac{(T_\infty - T_1)}{R_w} + \frac{(T_{1c} - T_1)}{R_c} + \frac{(T_2 - T_1)}{R_{conv}} + \frac{(T_3 - T_1)}{R_{conv}} + Q_1$$

(2) $$\rho\, V\, c_p\, \frac{dT_2}{dt} = 2\,\frac{(T_\infty - T_2)}{R_w} + \frac{(T_{2c} - T_2)}{R_c} + \frac{(T_4 - T_2)}{R_{conv}} + \frac{(T_1 - T_2)}{R_{conv}} +, Q_2$$

(3) $$\rho\, V\, c_p\, \frac{dT_3}{dt} = \frac{(T_\infty - T_3)}{R_w} + \frac{(T_{3c} - T_3)}{R_c} + \frac{(T_1 - T_3)}{R_{conv}} + \frac{(T_4 - T_3)}{R_{conv}} + \frac{(T_5 - T_3)}{R_{conv}} + Q_3$$

(4) $$\rho\, V\, c_p\, \frac{dT_4}{dt} = \frac{(T_\infty - T_4)}{R_w} + \frac{(T_{4c} - T_4)}{R_c} + \frac{(T_2 - T_4)}{R_{conv}} + \frac{(T_3 - T_4)}{R_{conv}} + \frac{(T_6 - T_4)}{R_{conv}} + Q_4$$

(5) $$\rho\, V\, c_p\, \frac{dT_5}{dt} = 2\,\frac{(T_\infty - T_5)}{R_w} + \frac{(T_{5c} - T_5)}{R_c} + \frac{(T_3 - T_5)}{R_{conv}} + \frac{(T_6 - T_5)}{R_{conv}} + Q_5$$

(6) $$\rho\, V\, c_p\, \frac{dT_6}{dt} = 2\,\frac{(T_\infty - T_6)}{R_w} + \frac{(T_{6c} - T_6)}{R_c} + \frac{(T_4 - T_6)}{R_{conv}} + \frac{(T_5 - T_6)}{R_{conv}} + Q_6$$

where: ρ – density, V – volume, c_p – specific heat at constant pressure, T – temperature, t – time, R – thermal resistance, Q – heat generation, ∞ – ambient, 1…6 – compartments, c – cooling surface of the TEM, w – wall, $conv$ – convection.

Equations (1–6) represent the energy conservation in each compartment neglecting the top and bottom surfaces for insulation and no direct contact of fluid in the box respectively. To calculate the heat transfer from the thermoelectric elements; TEM equations are used:

(7) $$Q_{ih} = \alpha\, I_i\, T_{ih} - k\,(T_{ih} - T_{ic}) + \frac{1}{2}\, I_i^2\, R_e = \frac{(T_{ih} - T_\infty)}{R_h}$$

(8) $$Q_{ic} = \alpha\, I_i\, T_{ic} - k\,(T_{ih} - T_{ic}) - \frac{1}{2}\, I_i^2\, R_e = \frac{(T_{ic} - T_{i1})}{R_c}$$

(9) $$V = I R_e + \alpha \Delta T$$

(10) $$P = V * I$$

where: α – seebeck coefficient, I_i – compartment current, T_{ih} – hot surface temperature, T_{ic} – cold surface temperature, k – thermal conductivity, R_e – TEM resistance, R_h – overall resistance from the hot side, R_c – overall resistance from the cold side.

The TEM used is TEC1-19908 and its characteristics are validated experimentally [40]. The TEM characteristics are $\alpha \cong 0.088$ V/K, $R_e \cong 2.38\ \Omega$ and $K \cong 0.8889$ W/K. Battery tank is 20×30×10 cm filled with water. Its assume, that each zone

has two TEM that are electrically connected in parallel, with maximum input current equal to 4 A.

Equation (7) and (8) written for each compartment in the battery box from i = 1 to 6. The Li-ion battery energy generation is given by:

$$Q_{ib} = I_b\,(E_{oc} - V) - I_b\,T_b\,\frac{dE_{oc}}{dT_b} \tag{11}$$

where: I_b – the battery current, E_{oc} – the open circuit potential, V – the cell potential.

Note that accurate identification of V and dE_{oc}/dT_b as a function of temperature and state of charge is a time-consuming laboratory work [30]. With the known TEM properties and current supplied, equations (7) and (8) are solved for T_{ih} and T_{ic} substituted back into equations (1) to (6) to find dT_i/dt for controlling process.

Control philosophy

NSB are a controlling scheme used in many applications such as multi-robotic formation control [35]. The NSB uses multiple behavioral tasks; the NSB is able to fulfill or partially fulfill each task according to their weight and priority [36-40]. Each task has value obtained as a function from the actual system states. The tasks variables are formulating a task space called Null-Space. Each system task has its own desired value that the system should maintain. Errors in the task level will be translated to controller behavioral commands. These control commands will be transformed back to actual system input commands. Referring to the multi-thermoelectric system used for BTMS; the basic concepts of the NSB are recalled by defining σ as the task variables that formulate a task space to be controlled:

$$\sigma = f(T) \tag{12}$$

where: $T \in R$ – the zones temperatures that are the system state space level, with the corresponding differential relationship:

$$\dot{\sigma} = \frac{\partial f(T)}{\partial T}\,v = J(T)\,v \tag{13}$$

where: $J \in R^{n\times m}$ – the configuration-dependent task Jacobian matrix, R^n – the system temperature changes.

Notice that *m* depends on the number of thermoelectric modules. As shown in Figure 5, the thermoelectric modules will act at differential level by inverting the mapping in equation (13). The proposed tasks $\sigma = f(T)$ constitute a collection (total zones average temperature). The difference in temperatures between the neighbor's zones and the average between the neighbor's zones are found by the following equation:

$$\sigma = f(T) = J \cdot T \tag{14}$$

where:

$$T = [T_1, T_2, T_3, T_4, T_5, T_6] \tag{15}$$

The desired temperature is $T_d(t)$. Starting from the desired temperature values and the corresponding $\sigma_d(t)$, the set of the task functions is found by:

$$\sigma_d = J \cdot T_d \tag{16}$$

where: J – the Jacobian matrix found as in equation (17).

$$\mathrm{J} = \begin{bmatrix} \frac{1}{6} & \frac{1}{6} & \frac{1}{6} & \frac{1}{6} & \frac{1}{6} & \frac{1}{6} \\ 1 & -1 & 0 & 0 & 0 & 0 \\ 1 & 0 & -1 & 0 & 0 & 0 \\ 0 & 1 & 0 & -1 & 0 & 0 \\ 0 & 0 & 1 & -1 & 0 & 0 \\ 0 & 0 & 1 & 0 & -1 & 0 \\ 0 & 0 & 0 & 1 & 0 & -1 \\ 0 & 0 & 0 & 0 & 1 & -1 \\ 0.4 & 0.4 & 0 & 0.2 & 0 & 0 \\ 0.4 & 0 & 0.4 & 0.2 & 0 & 0 \\ 0 & 0.4 & 0.2 & 0.4 & 0 & 0 \\ 0 & 0.1 & 0.4 & 0.4 & 0 & 0.1 \\ 0 & 0.1 & 0.4 & 0 & 0.4 & 0.1 \\ 0.1 & 0 & 0 & 0.4 & 0.1 & 0.4 \\ 0 & 0 & 0 & 0.2 & 0.4 & 0.4 \end{bmatrix} \tag{17}$$

According to the control schematic diagram in Figure 3, the system error signal is found in the task space level as:

$$E = \sigma_d - \sigma \tag{18}$$

where: E – the error value in the task space (Null space).

$$\dot{\sigma} = E \cdot K \tag{19}$$

where: K – the controller weight or gain matrix.

$$v = J^* \cdot \dot{\sigma} \tag{20}$$

where: J^* – the (pseudo)inverse.

It must be properly computed according to the dimension and the rank of the task Jacobian matrix. Then, the v will be the control command (TEMs current in this case) sent to the TEMs.

Simulation program

To solve the system predefined in Figure 1, governed by the system equations (1–6), with the battery load described in equation (11), a MATLAB program was created to solve equations (7) and (8) for T_c and T_h for each zone, then back substituted in equations (1–6) to find the change in temperature with respect to time for each zone within the battery system. The temperature change with respect to time was then integrated to give the new temperatures; these temperatures were then used to control the BTMS either by the PID or NSB control schemes. The NSB control scheme (Figure 3) is compared to PID control scheme in Figure 4.

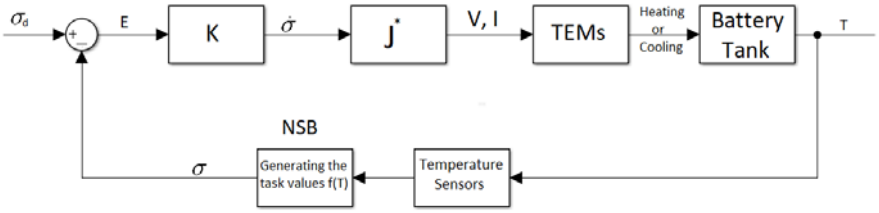

Fig. 3. The NSB controller diagram

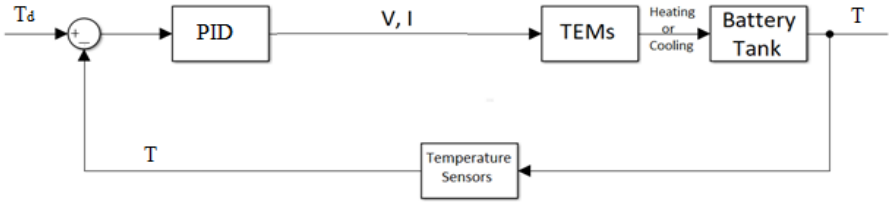

Fig. 4. The BTMS based on PID controller schematic diagram

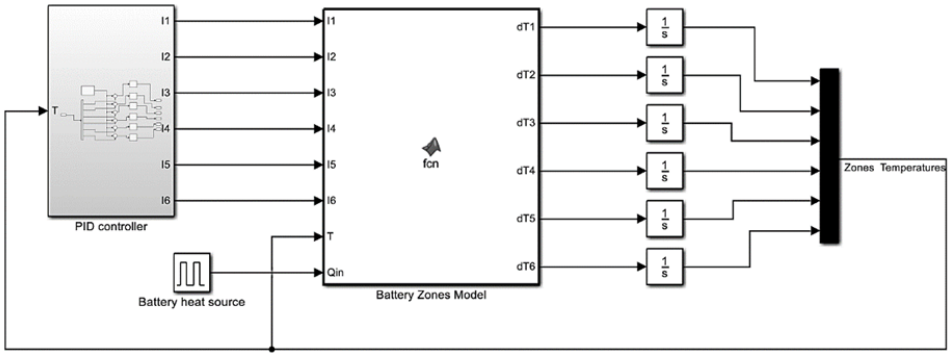

Fig. 5. MATLAB/Simulink using PID controller

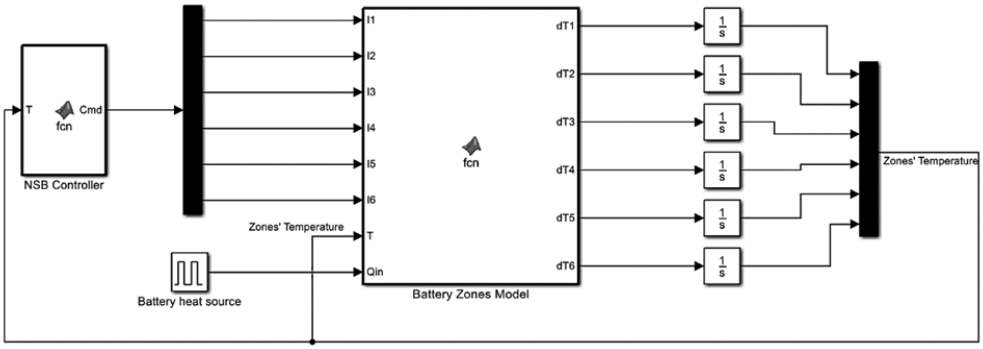

Fig. 6. MATLAB/Simulink using NSB controller

The new temperatures found from integrating the dT_i/dt were supplied to the PID controller shown in Figure 5. The PID controller block uses the input temperatures with the given set point (15+273) °C to manipulate the zones temperatures individually, so each zone has its own control loop. The PID controller parameters are $K_p = 10$, $K_i = 0.1$ and $K_d = 0$. The NSB controller uses a behavioral base mechanism to generate the task value, as shown in Figure 6, before it is resubstituted into the MATLAB program.

Results

To verify the effectiveness of the proposed NSB control system for BTMS, the simulation results for PID and NSB controllers were obtained using MATLAB/Simulink, which is considered as an effective software product in system engineering. The system initial temperature is set to 15 °C and surrounding temperature to 25 °C. At time 2000 s it is assumed, that zone 2 has been affected by a step heat generation within it equal to 70 W. This step heat generation increases the temperature of the zone and affects all other zones. The steady state temperatures and currents of all zones are presented in Table 1. It shows lower current consumptions using NSB controller, and much real temperatures in zones.

NSB controlling scheme allows for accurate behavioral control of the required task by relating the task with other variations in the system. A comparison between the power consumed to eliminate this heat generation using PID and NSB controllers is shown in Figure 7.

Table 1. Temperature current results during disturbance period at time 4000 second

Zone	PID temp., °C	PID Volts	PID curr., A	NSB temp., °C	NSB Volts	NSB curr., A
1	15.00	2.78	0.64	14.88	3.47	0.83
2	15.16	13.97	4.0	15.38	12.02	3.37
3	15.00	2.15	0.47	15.03	1.55	0.31
4	15.00	2.35	0.52	14.79	3.79	0.91
5	15.00	2.58	0.58	14.93	3.07	0.72
6	15.00	2.81	0.58	15.18	1.72	0.35

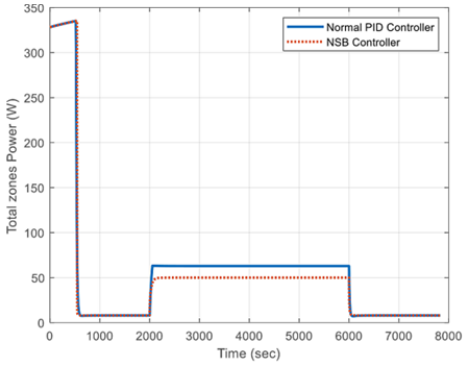

Fig. 7. Total power consumed in all zones using PID and NSB controllers

From Figure 7 it is clear, that the NSB controller uses power lower of 20% to control all the zones, that results in a better BTMS. Whereas the total current has been reduced due to the voltage difference and temperature difference between both cases. Figure 8 and Figure 9 shows the temperature variation in all zones versus time for both NSB and PID, respectively. The temperature of the NSB controller scheme is 0.8% higher than PID controlling scheme due to the collaborative mechanism. Its temperature returns to the set point in a faster time and shows a uniform variation. This uniform variation and quick return time results in a lower power consumption of NSB controller. Note that one penalty of using such method is that, there is a temperature variation occurred in the other zones. However, these variations will not have a negative effect since the lithium-ion battery is working on a temperature range 15–40 °C. Hence, it is acceptable to have a slightly lower temperatures deviation.

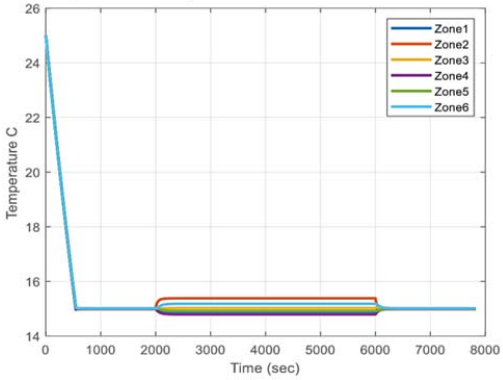

Fig. 8. The temperature variation in all zones versus time with NSB controller

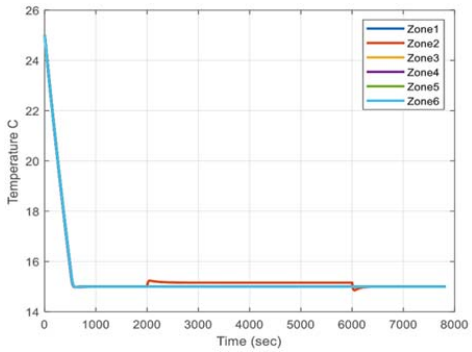

Fig. 9. The temperature variation in all zones versus time with PID controller

Freezing case

Figure 10 shows the freezing case the ambient temperature is 0 °C, and in the time 2000 a disturbance heat is active until 6000 second. It shows better energy consumption with NSB over the PID. The current in Table 2 shows negative signs; this is due to the heating functionality of the TEM.

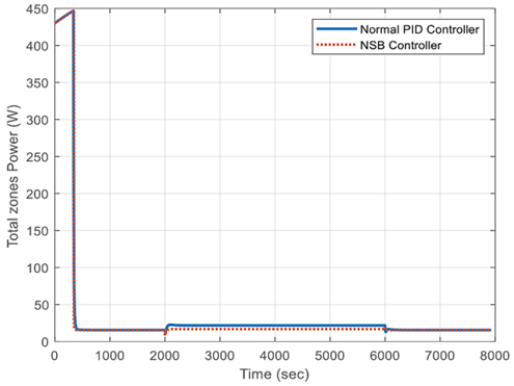

Fig. 10. Total power consumed in all zones using PID and NSB controllers with freezing ambient temperature

Table 2. Temperature current results with freezing case during disturbance period at time 4000 second

Zone	PID temp., °C	PID Volts	PID curr., A	NSB temp., °C	NSB Volts	NSB curr., A
1	15.00	-3.64	-0.79	14.88	-3.03	-0.63
2	15.53	5.43	1.67	15.27	4.08	1.28
3	15.00	-3.09	-0.65	15.03	-3.60	-0.77
4	15.00	-3.09	-0.65	14.84	-2.03	-0.39
5	15.00	-3.64	-0.79	14.91	-3.26	-0.69
6	15.00	-3.64	-0.79	15.13	-4.23	-0.93

From the Figure 10, the energy consumption of NSB controller is 22% less, compared with PID controller. It worth to note that the TEM at zone 2 show positive volts and current direction since a disturbance heat source is active at this zone, thus the system still needs cooling.

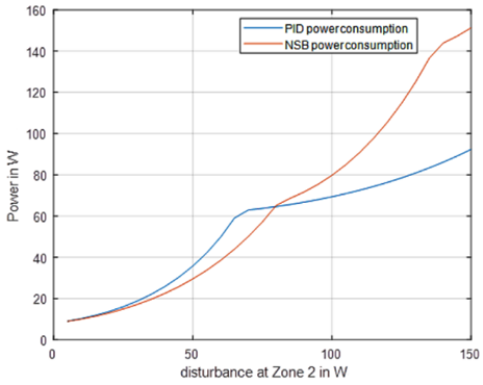

Fig. 11. Power consumption for both PID and NSB controllers at zone 2 with 25 °C ambient temperature

Power consumption

The power consumption for both PID and NSB controllers has been investigated with disturbance load. Figure 11 shows

that the NSB controller consumes lower power than PID controller until the disturbance load reach a maximum at almost 75 W, where the current consumed by the TEM reaches its maximum value of 4 A. At this stage the PID controller becomes better than NSB, because the TEM is no more able to exceed the allowable current. Table 3 shows the temperature and current results for freezing case with disturbance heat load 150 W, which exceeds the maximum current at zone 2.

Table 3. Temperature and current results with freezing case during disturbance period at time 4000 s and 150 W disturbance at zone 2

Zone	PID temp., °C	PID Volts	PID curr., A	NSB temp., °C	NSB Volts	NSB curr., A
1	15.00	8.15	2.17	13.85	10.92	3
2	18.80	13.86	4	17.79	13.89	4
3	15.00	2.15	0.4698	14.98	-0.89	-0.32
4	15.00	7.59	2	13.93	14	4
5	15.00	2.58	0.58	14.61	4.87	1.21
6	15.00	2.58	0.58	15.85	-1.40	-0.44

Conclusions

In the simulation research, a NSB controller for EV-BTMS has been implemented to control the cells temperatures for longer life and safe operation of the EV Li-ion batteries. The NSB controller uses different behavioral patterns to control the thermal system, which results in a highly suitable controlling mechanism for the specified application. The results of NSB controller compared to PID, shows: (i) to achieve of 20% reduction in the consumed power, (ii) faster temperature return to the set point, and (iii) a more uniform behavior in controlling the temperature of the battery cells. The method used increases the life of batteries by keeping them at optimum operating conditions, as well the life of TEMs used by subjecting them to a lower current, finally affecting to reduce the energy consumed.

Acknowledgements: *This article was supported by the Lublin University of Technology (Grant No. FD-20/IS-6/002).*
The authors are appreciative of the financial support provided by Applied Science Private University, Jordan.

Authors: *Dr Mohammad Tariq Nasir, Department of Mechanical and Industrial Engineering, Applied Science Private University, P.O. Box 166, 11931, Amman, Jordan, e-mail: mo_nasir@asu.edu.jo; Dr Nabil Beithou, Department of Mechanical Engineering, Tafila Technical University, P.O. Box 179, 66110, Tafila, Jordan, e-mail: nabil.betthou@ttu.edu.jo; Prof. dr hab. inż. Gabriel Borowski, Faculty of Environmental Engineering, Lublin University of Technology, ul. Nadbystrzycka 40B, 20-618 Lublin, Poland, e-mail: g.borowski@pollub.pl; Dr Sameh Alsaqoor, Department of Mechanical Engineering, Tafila Technical University, P.O. Box 179, 66110, Tafila, Jordan, e-mail: sameh@wp.pl*

REFERENCES

[1] U.S. Information Administration, Monthly Energy Review, Table 2.1, April 2021
[2] Gramling C., How electric vehicles offered hope as climate challenges grew. *ScienceNews*, 200 (2021), 11 (Access 2022.03.10: https://www.sciencenews.org/article/electric-vehicles-cars-climate-change-challenges-2021)
[3] International Energy Agency Special Report, 2021. Net Zero by 2050: A Road Map for Global Energy Sector. IEA, Paris (Access 2022.03.10: https://www.iea.org/reports/net-zero-by-2050)
[4] Esfahanian V., Renani S.A., Nehzati H., Mirkhani N., Esfahanian M., Yaghoobi O., Safaei A., Design and simulation of air cooled battery thermal management system using thermoelectric for a hybrid electric bus. Proceedings of the FISITA 2012 World Automotive Congress (2012), 463–4730. https://doi.org/10.1007/978-3-642-33777-2_37
[5] Bandhauer T.M., Garimella S., Fuller T.F., A critical review of thermal issues in lithium-ion batteries. *Journal of The Electrochemical Society,* 158 (2011), 3, 1-25, https://doi.org/10.1149/1.3515880
[6] Zhao L., Yang Z., Wang L., Investigation on the non-uniform temperature distribution of large-diameter concrete silos under solar radiation. *Mathematical Problems in Engineering* (2018), Article ID 5304974. https://doi.org/10.1155/2018/5304974
[7] Rao Z., Wang S., A review of power battery thermal energy management. *Renewable and Sustainable Energy Reviews* 15 (2011), 9, 4554-4571. https://doi.org/10.1016/j.rser.2011.07.096
[8] Giuliano M.R., Advani S.G., Prasad A.K., Thermal analysis and management of lithium–titanate batteries. *Journal of Power Sources* 196 (2011), 15, 6517–6524. https://doi.org/10.1016/j.jpowsour.2011.03.09
[9] An Z., Jia L., Ding Y., Dang C., Li X., A review on lithium-ion power battery thermal management technologies and thermal safety. *Journal of Thermal Science* 26 (2017), 5, 391–412. https://doi.org/10.1007/s11630-017-0955-2
[10] Li X., Zhong Z., Luo J., Wang Z., Yuan W., Zhang G., … Yang C., Experimental Investigation on a thermoelectric cooler for thermal management of a Lithium-Ion battery module. *International Journal of Photoenergy* (2019), Article ID 3725364. https://doi.org/10.1155/2019/3725364
[11] Javani N., Dincer I., Naterer G.F., Yilbas B.S., Heat transfer and thermal management with PCMs in a Li-ion battery cell for electric vehicles. *International Journal of Heat and Mass Transfer* 72 (2014), 690–703. https://doi.org/10.1016/j.ijheatmasstransfer.2013.12.076
[12] Jiang G., Huang J., Fu Y., Cao M., Liu M., Thermal optimization of composite phase change material/expanded graphite for Li-ion battery thermal management. *Applied Thermal Engineering* 108, (2016), 1119–1125. https://doi.org/10.1016/j.applthermaleng.2016.07.197
[13] Wu W., Yang X., Zhang G., Chen K., Wang S., Experimental investigation on the thermal performance of heat pipe-assisted phase change material based battery thermal management system. *Energy Conversion and Management* 138 (2017), 486–492. https://doi.org/10.1016/j.enconman.2017.02.022
[14] Wilke S., Schweitzer B., Khateeb S., Al-Hallaj S., Preventing thermal runaway propagation in lithium-ion battery packs using a phase change composite material: An experimental study. *Journal of Power Sources* 340 (2017), 51–59. https://doi.org/10.1016/j.jpowsour.2016.11.018
[15] Sefidan A.M., Sojoudi A., Saha S.C., Nanofluid-based cooling of cylindrical lithium-ion battery packs employing forced air flow. *International Journal of Thermal Sciences* 117 (2017), 44–58. https://doi.org/10.1016/j.ijthermalsci.2017.03.006
[16] Yang X.-H., Tan S.-C., Liu J., Thermal management of Li-ion battery with liquid metal. *Energy Conversion and Management* 117, (2016), 577–585. https://doi.org/10.1016/j.enconman.2016.03.054
[17] Al-Zareer M., Dincer I., Rosen M.A., Electrochemical modeling and performance evaluation of a new ammonia-based battery thermal management system for electric and hybrid electric vehicles. *Electrochimica Acta* 247, (2017), 171–182. https://doi.org/10.1016/j.electacta.2017.06.162
[18] Chen, K., Song, M., Wei, W., & Wang, S., Structure optimization of parallel air-cooled battery thermal management system with U-type flow for cooling efficiency improvement. *Energy* 145 (2018), 603–613. https://doi.org/10.1016/j.energy.2017.12.110
[19] Song W., Chen M., Bai F., Lin S., Chen Y., Feng Z., Non-uniform effect on the thermal/aging performance of lithium-ion pouch battery. *Applied Thermal Engineering* 128, (2018) 1165–1174. https://doi.org/10.1016/j.applthermaleng.2017.09.090
[20] Situ W., Zhang G., Li X., Yang X., Wei C., Rao M., … Wu W., A thermal management system for rectangular $LiFePO_4$ battery

module using novel double copper mesh-enhanced phase change material plates. *Energy* 141 (2017), 613–623. https://doi.org/10.1016/j.energy.2017.09.083
[21] Alaoui C., Solid-state thermal management for Lithium-Ion EV batteries. *IEEE Transactions on Vehicular Technology* 62 (2013), 98–107. https://doi.org/10.1109/tvt.2012.2214246
[22] Salameh Z.M., Alaoui C., Modeling and simulation of a thermal management system for electric vehicles. Proceedings of 29th Annual Conference of the IEEE Industrial Electronics Society (2003), Article ID 7954269. https://doi.org/10.1109/iecon.2003.1280100
[23] Liu Y., Yang S., Guo B., Deng C., Numerical analysis and design of thermal management system for Lithium-Ion battery pack using thermoelectric coolers. *Advances in Mechanical Engineering* 6 (2014), Article ID 852712. https://doi.org/10.1155/2014/852712
[24] Jiang G., Huang J., Liu M., Cao M., Experiment and simulation of thermal management for a tube-shell Li-ion battery pack with composite phase change material. *Applied Thermal Engineering*, 120 (2017), 1-9. https://doi.org/10.1016/j.applthermaleng.2017.03.107
[25] Doshi M., Udawant S., Devkule D., Gadekar S., Microcontroller based thermoelectric cooling for electric vehicle battery charging application. Proceedings of 2nd International Conference on Communication & Information Processing (ICCIP) 2020, http://dx.doi.org/10.2139/ssrn.3645352
[26] Samanta A., Williamson, S.S., A comprehensive review of lithium-ion cell temperature estimation techniques applicable to health-conscious fast charging and smart battery management systems. *Energies* 14 (2021), 18, 5960. https://doi.org/10.3390/en14185960
[27] Chikaraishi R., Deng M., Operator-based nonlinear control of calorimetric system actuated by Peltier device. *Machines* 9 (2021), (8), 174. https://doi.org/10.3390/machines9080174
[28] Wang B., Fernandez J.H., Massoud A., A wireless battery temperature monitoring system for electric vehicle charging. Proceedings of IEEE Sensors (2019), 1-4. https://doi.org/10.1109/sensors43011.2019.8956733
[29] Alahmer A., Khalid M.B., Beithou N., Borowski G., Al Hendi H., Alsaqoor S., An experimental investigation into improving the performance of thermoelectric generators. *Journal of Ecological Engineering* 23 (2022), 3, 100-108. https://doi.org/10.12911/22998993/145457
[30] Lyu Y., Siddique A.R.M., Majid S.H., Biglarbegian M., Gadsden S.A., Mahmud S., Electric vehicle battery thermal management system with thermoelectric cooling. *Energy Reports* 5 (2019), 822-827. https://doi.org/10.1016/j.egyr.2019.06.016
[31] Zhang X., Li Z., Luo L., Fan Y., Du Z., A review on thermal management of lithium-ion batteries for electric vehicles. *Energy* 238 (2022), Article ID 121652. https://doi.org/10.1016/j.energy.2021.121652
[32] Arrichiello F., Chiaverini S., Indiveri G., Pedone P., The null-space-based behavioral control for mobile robots with velocity actuator saturations. *The International Journal of Robotics Research* 29 (2010),10, 1317-1337. https://doi.org/10.1177/0278364909358788
[33] Sundayani, Sinulingga D.F., Prasetyawati F.M., Palebangan F.M., Suhendi A., Ajiwiguna T.A., … Fathonah I.W., PID temperature controlling of thermoelectric based cool box. Proceedings of International Conference on Control, Electronics, Renewable Energy and Communications (ICCREC' 2017), 236-240. https://doi.org/10.1109/iccerec.2017.8226671
[34] Saleet H., Smart solution for enhancing storage location assignments in WMS using genetic algorithm. *International Journal of Engineering Research and Technology* 13 (2020), 11, 3456-3463. (Access 2022.03.10: http://www.irphouse.com)
[35] Liu Y., Yang S., Guo B., Deng C., Numerical analysis and design of thermal management system for lithium ion battery pack using thermoelectric coolers. *Advances in Mechanical Engineering* 6 (2014), Article ID 852712. https://doi.org/10.1155/2014/852712
[36] Arrichiello F., Chiaverini S., Fossen T., Formation control of underactuated surface vessels using the null-space-based behavioral control. Proceedings of IEEE/RSJ International Conference on Intelligent Robots and Systems (2006). https://doi.org/10.1109/iros.2006.282477
[37] Quintana-Carapia G., Benítez-Read J.S., Segovia-De-Los-Ríos J.A., Null space based behavior control applied to robot formation. Proceedings of IEEE World Automation Congress (2012), 1-6 (Access 2022.03.10: https://ieeexplore.ieee.org/abstract/document/6321275)
[38] Nemec B., Žlajpah L., Omrčen D., Comparison of null-space and minimal null-space control algorithms. *Robotica* 25 (2007), 5, 511-520. https://doi.org/10.1017/s0263574707003402
[39] Antonelli G., Arrichiello F., Chiaverini S., The NSB control: A behavior-based approach for multi-robot systems. *Paladyn*, *Journal of Behavioral Robotics* 1 (2010), 48-56. https://doi.org/10.2478/s13230-010-0006-0
[40] Nasir M.T., Afaneh D., Abdallah S., High productivity thermoelectric based distiller. *Desalination and Water Treatment* 206 (2020), 125-132. https://doi.org/10.5004/dwt.2020.26295